Inorg. Chem. **2002**, *41*, 6387–6396

A Superior Polypyridine Ligand for Platinum(II) Lumaphors. Methyl Substituents with a Large Stereoelectronic Influence

Jeffrey J. Moore, John J. Nash, Phillip E. Fanwick, and David R. McMillin*

Department of Chemistry, Purdue University, 560 Oval Drive, West Lafayette, Indiana 47907-2038

Received August 2, 2002

This research deals with the synthesis and characterization of a new series of platinum(II) polypyridine complexes that incorporate a relatively rigid and hydrophobic ligand. The parent complex Pt(php)Cl$^+$, where php denotes 2-(2′-pyridyl)-1,10-phenanthroline, resembles Pt(trpy)Cl$^+$, where trpy denotes 2,2′:6′,2″-terpyridine, but is photoluminescent in solution. Hence php derivatives should prove to be superior tags and/or spectroscopic probes for biological systems. A theoretical analysis reveals some of the advantages of php over trpy as a platform. Due to a ligand π system with a relatively small HOMO–LUMO gap, the emission from Pt(php)Cl$^+$ exhibits significant vibrational structure and a mixed $^3\pi$–π^*/^{3}d–π^* orbital parentage. In deoxygenated dichloromethane solution the php complex exhibits an emission quantum yield of 3.1×10^{-3} and an excited-state lifetime of 0.23 μs at room temperature. However, methyl groups have an unusually strong stereoelectronic influence, particularly at the 5,6-positions of the phenanthroline moiety. The platinum(II) complex with 2-(2′-pyridyl)-3,5,6,8-tetramethyl-1,10-phenanthroline is the best emitter with an emission yield of 0.055 and a lifetime of 9.3 μs in dichloromethane. Strongly donating solvents like dimethylformamide are potent quenchers of the emission. The methods of characterization used include absorption and emission spectroscopies, electrochemistry, and, in the case of [Pt{2-(2′-pyridyl)-4,7-dimethyl-1,10-phenanthroline}Cl]O_3SCF_3, X-ray crystallography. Another intriguing finding is that methyl substituents have preferred orientations with respect to the phenanthroline ligand.

Introduction

The goal of this research has been to develop new luminescent platinum(II) polypyridine complexes incorporating a rigid ligand framework, substantial hydrophobic character, and compatibility with a variety of solvents including water. Interest in the chemistry and spectroscopy of the archetypical Pt(trpy)Cl$^+$ system, where trpy denotes 2,2′:6′,2″-terpyridine (Chart 1), continues for a number of reasons.[1] One is that the complex binds covalently to biological macromolecules by means of substitution of the relatively labile chloride ligand.[2,3] Intercalation into double-helical DNA is also feasible because of the planar coordination geometry and the presence of the aromatic polypyridine ligand.[4,5] Metal-to-ligand charge-transfer (MLCT) absorption bands that occur in the vicinity of 400 nm provide a useful spectral handle. Unfortunately, even though Pt(trpy)Cl$^+$ is luminescent in the solid state and in low-temperature glasses,[6,8,9] the complex gives essentially no photoluminescence in fluid solution because nonradiative decay via thermally accessible d−d excited states is quite efficient.[7] Luminescent derivatives of Pt(trpy)Cl$^+$ have, however, been identified. For example, Pt(trpy)(OH)$^+$ is luminescent, but only in weakly basic organic solvents.[7] Emission measurements are useful for DNA-binding studies because the

Chart 1

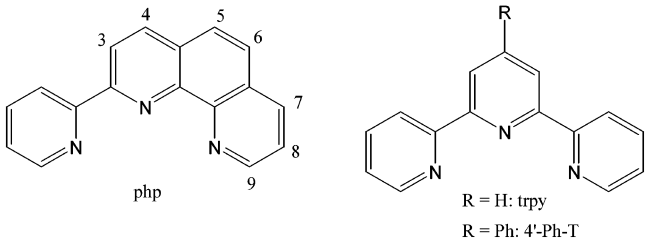

* To whom all correspondence should be addressed. E-mail: mcmillin@purdue.edu.

(1) McMillin, D. R.; Moore, J. J. *Coord. Chem. Rev.* **2002**, *229*, 113−121.
(2) Jennette, K. W.; Lippard, S. J.; Vassiliades, G. A.; Bauer, W. R. *Proc. Natl. Acad. Sci. U.S.A.* **1974**, *71*, 3839−3843.
(3) Ratilla, E. M. A.; Brothers, H. M.; Kostic, N. M. *J. Am. Chem. Soc.* **1987**, *109*, 4592−4599.

10.1021/ic025922c CCC: $22.00
Published on Web 10/31/2002

hydroxide complex does not emit in aqueous solution but becomes luminescent upon intercalating into a DNA host.[5] However, in the presence of guanine bases, electron-transfer quenching can be very efficient.[5] Incorporation of electron-rich substituents, like dimethylamine or 1-pyrene, at the 4′-position of the trpy ligand also yields derivatives that can have microsecond-lived emissions in noncoordinating media.[10−12] Even a simple phenyl substituent has an important effect. Thus, Pt(4′-Ph-T)Cl^+, where 4′-Ph-T denotes 4′-phenyl-2,2′:6′,2″-terpyridine, exhibits emission with a lifetime of 85 ns in room-temperature dichloromethane (DCM).[11,12] The presence of the phenyl substituent provides for an expanded π system, a lower energy MLCT state, and less efficient deactivation via d−d excited states. However, it is also possible that the intrinsic excited-state lifetime increases because the ligand is less prone to distortion.[13]

The results described below show that 2-(2′-pyridyl)-1,10-phenanthroline (php in Chart 1) is a superior ligand for a platinum(II)-based lumaphore. Thus, Pt(php)Cl^+ exhibits an emission signal with a lifetime of 230 ns in DCM solution at room temperature; more impressive, analogues bearing only methyl substituents can have lifetimes of many microseconds. The structure of a 4,7-dimethyl complex shows that there is less dispersion in the Pt−N bonds of a php complex than in the trpy analogue and that coordinated php is essentially planar. The rigidity of the php ligand may restrict excited-state distortions and thereby enhance the emission relative to that of the trpy analogue. However, an even more telling observation is that the emission from the php complex originates in an excited state with not only ^{3}d−π* (CT) but significant $^3\pi-\pi^*$ (intraligand) character as well. Introducing methyl substituents affects the $^3\pi-\pi^*/^3$d−π* mix much like the solvent tuning that has been reported for Ir(III) systems.[14] The solvent sensitivity of the emission from php-based systems suggests that the platinum complexes will be useful as spectroscopic reporter probes and in sensing studies.

Experimental Section

Materials. The $ZnCl_2$ and $Fe(NH_4)_2(SO_4)_2\cdot 6H_2O$ compounds came from Mallinckrodt, while K_2PtCl_4 came from Johnson and Matthey Pharmaceuticals. Aldrich Chemical Co. was the vendor for 1,10-phenanthroline, 4,7-dimethyl-1,10-phenanthroline, 5,6-dimethyl-1,10-phenanthroline, 3,4,7,8-tetramethyl-1,10-phenanthroline, 2-bromopyridine, 1,5-cyclooctadiene, *n*-butyllithium (as a 2 M solution in cyclohexane), butyronitrile, and ferrocene. The Na[TPFB]·$n H_2O$[10] (TPFB = tetrakis[3,5-bis(trifluoromethyl)phenyl]-borate), [Pt(4′-Ph-T)Cl]TFPB[12] (4′-Ph-T = 4′-phenyl-2,2′:6′,2″-terpyridine), and Pt(trpy)Cl^+ [7] (trpy = 2,2′:6′,2″-terpyridine) were available from previous studies. Exciton supplied the laser dyes. Reagent-grade chemicals sufficed for synthetic purposes, but the purification of tetrabutylammonium hexafluorophosphate (TBAH) electrolyte required two recrystallizations from ethanol. For spectral studies high-purity-grade acetonitrile (MeCN), dichloromethane (DCM), and toluene (MePh) came from VWR under the label of Burdick and Jackson. The ^{1}H NMR solvent $CDCl_3$ was a product of Cambridge Isotope Labs.

Syntheses. Literature methods yielded 3,5,6,8-tetramethyl-1,10-phenanthroline ligand,[15] Pt(COD)Cl_2[16] (COD = 1,5-cyclooctadiene), and the various Zn(php)Cl_2 derivatives.[17,18] Preparations of [Pt(php)Cl]Cl and complexes with related ligands followed the method of Annibale et al.,[19] with Pt(COD)Cl_2 as the starting material. It was possible to exchange the counterion by simple metathesis procedures carried out in DCM. A metathesis procedure also yielded the tetramethylammonium salt of the TFPB anion. Fe(php)$_2^{2+}$ and iron(II) complexes of related ligands were made in situ by combining $Fe(NH_4)_2(SO_4)_2\cdot 6H_2O$ with 2 equiv of the appropriate polypyridine ligand in deionized water.

The following procedure for the preparation of 2-(2′-pyridyl)-1,10-phenanthroline (php) incorporates several literature methods.[20−22] Analogous procedures yield the various methylated forms. Addition of a stoichiometric amount of *n*-butyllithium to a solution of 2-bromopyridine in dry tetrahyrdofuran (THF) at −78 °C under Ar gave a red solution. After stirring for 15 min, a transfer of 1.2 equiv of the resulting lithium reagent, via cannula, to a solution of 1,10-phenathroline in dry THF at −78 °C, also under Ar, produced another deep red solution. After the mixture was stirred for 2 h, water was added to quench any unreacted lithium reagent and organics were extracted into DCM. All organics were combined and rearomatized by combining with an excess of the oxidant MnO_2. After incubating for 2 h, the solution was filtered, dried with Na_2SO_4, and concentrated to a yellow oil. The crude product was purified by column chromatography on alumina, with THF/hexanes (5/1) as the eluent. A white solid was obtained from the column after evaporation of solvents. Further purification was accomplished via recrystallization from 1:1 (v/v) DCM/hexanes. Analytical data for the various php ligands follow.

2-(2′-Pyridyl)-1,10-phenanthroline (php). Anal. Calcd for $C_{17}H_{11}N_3\cdot {}^1/_4(CH_2Cl_2)$: 74.26 %C, 4.04 %H, 15.02 %N. Found: 74.38 %C, 4.16 %H, 15.08 %N. ^{1}H NMR in $CDCl_3$ (in ppm): 9.25 (dd, 1H), 9.00 (d, 1H), 8.80 (d, 1H), 8.75 (m, 1H), 8.38 (d, 1H), 8.25 (dd, 1H), 7.92 (td, 1H), 7.82 (m, 2H), 7.65 (m, 1H), 7.38 (m, 1H).

(4) Sundquist, W. I.; Lippard, S. J. *Coord. Chem. Rev.* **1990**, *100*, 293−322.
(5) Peyratout, C. S.; Aldridge, T. K.; Crites, D. K.; McMillin, D. R. *Inorg. Chem.* **1995**, *34*, 4484−4489.
(6) Yip, H. K.; Cheng, L. K.; Cheung, K. K.; Che, C. M. *J. Chem. Soc., Dalton Trans.* **1993**, 2933−2938.
(7) Aldridge, T. K.; Stacy, E. M.; McMillin, D. R. *Inorg. Chem.* **1994**, *33*, 722−727.
(8) Buchner, R.; Field, J. S.; Haines, R. J.; Cunningham, C. T.; McMillin, D. R. *Inorg. Chem.* **1997**, *36*, 3952−3956.
(9) Bailey, J. A.; Hill, M. G.; Marsh, R. E.; Miskowski, V. M.; Schaefer, W. P.; Gray, H. B. *Inorg. Chem.* **1995**, *34*, 4591−4599.
(10) Crites, D. K.; Cunningham, C. T.; McMillin, D. R. *Inorg. Chim. Acta* **1998**, *273*, 346−353.
(11) Michalec, J. F.; Bejune, S. A.; McMillin, D. R. *Inorg. Chem.* **2000**, *39*, 2708−2709.
(12) Michalec, J. F.; Bejune, S. A.; Cuttell, D. G.; Summerton, G. C.; Gertenbach, J. A.; Field, J. S.; Haines, R. J.; McMillin, D. R. *Inorg. Chem.* **2001**, *40*, 2193−2200.
(13) Strouse, G. F.; Schoonover, J. R.; Duesing, R.; Boyde, S.; Jones, W. E.; Meyer, T. J. *Inorg. Chem.* **1995**, *34*, 473−487.
(14) Crosby, G. A. *Acc. Chem. Res.* **1975**, *8*, 231−238.
(15) Case, F. H. *J. Am. Chem. Soc.* **1948**, *70*, 3994−3996.
(16) McDermott, J. X.; White, J. F.; Whitesides, G. M. *J. Am. Chem. Soc.* **1976**, *98*, 6521−6528.
(17) Hill, M. G.; Bailey, J. A.; Miskowski, V. M.; Gray, H. B. *Inorg. Chem.* **1996**, *35*, 4585−4590.
(18) Douglas, J. E.; Wilkins, C. *Inorg. Chim. Acta* **1969**, *3*, 635−638.
(19) Annibale, G.; Brandolisio, M.; Pitteri, B. *Polyhedron* **1995**, *14*, 451−453.
(20) Barigelletti, F.; Ventura, B.; Collin, J. P.; Kayhanian, R.; Gavina, P.; Sauvage, J. P. *Eur. J. Inorg. Chem.* **2000**, 113−119.
(21) Malmberg, H.; Nilsson, M. *Tetrahedron* **1986**, *42*, 3981−3986.
(22) Collin, J. P.; Gavina, P.; Sauvage, J. P.; De Cian, A.; Fischer, J. *Aust. J. Chem.* **1997**, *50*, 951−957.

2-(2′-Pyridyl)-4,7-dimethyl-1,10-phenanthroline (4,7-Me_2-php). Anal. Calcd for $C_{19}H_{15}N_3$: 79.98 %C, 5.30 %H, 14.73 %N. Found: 79.74 %C, 5.18 %H, 14.61 %N. ^{1}H NMR in $CDCl_3$ (in ppm): 9.12 (d, 1H), 9.05 (d, 1H), 8.75 (m, 1H), 8.68 (s, 1H), 8.09 (m, 2H), 7.92 (dt, 1H), 7.50 (d, 1H), 7.38 (m, 1H), 2.90 (s,3H), 2.80 (s, 3H).

2-(2′-Pyridyl)-5,6-dimethyl-1,10-phenanthroline (5,6-Me_2-php). Anal. Calcd for $C_{19}H_{15}N_3 \cdot 1.25H_2O$: 74.12 %C, 5.72 %H, 13.64 %N. Found: 74.18 %C, 5.47 %H, 13.58 %N. ^{1}H NMR in $CDCl_3$ (in ppm): 9.20 (dd, 1H), 9.04 (d, 1H), 8.78−8.74 (m, 2H), 8.58 (d, 1H), 8.48 (dd, 1H), 7.92 (td, 1H), 7.66 (m, 1H), 7.38 (m, 1H), 2.75 (s, 3H), 2.70, (s, 3H).

2-(2′-Pyridyl)-3,4,7,8-tetramethyl-1,10-phenanthroline (3,4,7,8-Me_4-php). Anal. Calcd for $C_{21}H_{19}N_3 \cdot {}^1/_4(H_2O)$: 79.33 %C, 6.18 %H, 13.22 %N. Found: 79.53 %C, 6.13 %H, 13.24 %N. ^{1}H NMR in $CDCl_3$ (in ppm): 8.97 (s, 1H), 8.70 (m, 1H), 8.0−8.12 (m, 3H), 7.90 (td, 1H), 7.35 (m, 1H), 2.78 (s, 3H), 2.7 (s, 3H), 2.58 (s, 3H), 2.52 (s, 3H).

2-(2′-Pyridyl)-3,5,6,8-tetramethyl-1,10-phenanthroline (3,5,6,8-Me_4-php). Anal. Calcd for $C_{19}H_{15}N_3 \cdot {}^1/_4(H_2O)$: 79.34 %C, 6.18 %H, 13.21 %N. Found: 79.06 %C, 6.18 %H, 12.98 %N. ^{1}H NMR in $CDCl_3$ (in ppm): 8.95 (s, 1H), 8.72 (d, 1H), 8.32 (s, 1H), 8.22 (m, 2H) 7.90 (dt, 1H), 7.34 (m, 1H), 2.78 (s, 3H), 2.74 (s, 3H), 2.70 (s, 3H), 2.6 (s, 3H).

Preparation of [Pt(php)Cl]TFPB. To obtain the php complex, one combines 100 mg of the php ligand (dissolved in a small volume of acetone) with a suspension of 1 molar equiv of Pt(COD)-Cl_2 in aqueous 0.05 M 2-(*N*-morpholine)ethanesulfonic acid. The solution clarifies and turns yellow upon heating. After filtration and the addition of NaCl(aq), Pt(php)Cl^+ precipitates as a red chloride salt. A solution of the TFPB salt forms with the gentle heating of the aforementioned solid in DCM containing a substoichiometric amount (ca. 0.9 equiv) of Na[TFPB]·*n*H_2O. After removal of the insoluble materials, evaporation of the solvent yields the desired yellow solid. The final purification step involves recrystallization from 1:1 DCM/hexane. Analogous procedures yield the related compounds involving methylated forms of php. See below for analytical data.

[Pt(php)Cl]TFPB. Anal. Calcd ($C_{49}H_{23}N_3ClF_{24}BPt$): 43.56 %C, 1.72 %H, 3.11 %N. Found: 43.73 %C, 1.99 %H, 2.88 %N.

[Pt(4,7-Me_2-php)Cl]TFPB·0.5(CH_2Cl_2). Anal. Calcd ($C_{51.5}H_{28}N_3Cl_2F_{24}BPt$): 43.48 %C, 1.98 %H, 2.95 %N. Found: 43.54 %C, 2.02 %H, 2.76 %N.

[Pt(5,6-Me_2-php)Cl]TFPB. Anal. Calcd ($C_{53}H_{31}N_3ClF_{24}BPt$): 44.42 %C, 1.97 %H, 3.05 %N. Found: 44.24 %C, 2.17 %H, 2.76 %N.

[Pt(3,4,7,8-Me_4-php)Cl]TFPB. Anal. Calcd ($C_{53}H_{31}N_3ClF_{24}BPt$): 45.24 %C, 2.22 %H, 2.99 %N. Found: 45.21 %C, 2.24 %H, 2.93 %N.

[Pt(3,5,6,8-Me_4-php)Cl]TFPB·${}^1/_2$(CH_2Cl_2). Anal. Calcd ($C_{53}H_{31}N_3ClF_{24}BPt \cdot {}^1/_2(CH_2Cl_2)$): 44.50 %C, 2.22 %H, 2.76 %N. Found: 44.65 %C, 2.05 %H, 2.48 %N.

Methods. A series of freeze−pump−thaw cycles removed dioxygen prior to luminescence measurements. For steady-state emission studies, the slit settings were 10 nm for both the excitation and emission beams. The excitation wavelength was 420 nm, and a 440 nm long-wave-pass filter removed the scattered light. The source of the instrumental correction factors has been described,[23] and the conversion from wavelength to an emission-energy scale was standard.[24] The method of Parker and Rees[25] allowed the estimation of emission quantum yields at 25 °C with $Ru(bpy)_3^{2+}$ in water as the standard ($\phi = 0.042$).[26] For the lifetime studies, there was a neutral density filter between the sample and the laser and a 525 nm long-wave-pass filter between the sample and the detector. The excitation wavelength was usually 420 nm. Residual plots verified that a single-exponential model was adequate to fit the emission decay data.

In the electrochemical studies the working electrode was a gold button, while the auxiliary electrode was a platinum wire. The experimental setup involved an aqueous Ag/AgCl (3 M NaCl) reference electrode, but it is more useful to quote potentials versus ferrocene in the actual working medium. The potentials reported are the mean of the cathodic ($E_{p,c}$) and anodic ($E_{p,a}$) peaks in the cyclic voltammogram. The scan rate for all scans was 50 mV s^{-1}, and the electrolyte solution was 0.1 M TBAH in DMF. A simple purge of dinitrogen gas sufficed to deaerate the sample.

Instrumentation. The absorption spectrometer was a Varian Cary 100 Bio instrument, and the spectrofluorometer was an SLM-Aminco SPF-500C. The cryostat was an Oxford Instruments model DN1704 liquid-nitrogen-cooled system complete with an Oxford Instruments model ITC4 temperature controller. A description of the laser excitation system and photomultiplier detector appears in the literature.[27] The cyclic voltammetry unit was a model CV-27 from Bioanalytical Systems, Inc., connected to a Hewlett-Packard 7015B XY chart recorder. The ^{1}H NMR spectrometer was a Varian Gemini 200 MHz. The Nonius KappaCCD package served for the preliminary examination of the crystals and data collection with Mo Kα radiation ($\lambda = 0.71073$ Å). The computer for all structure refinements was an AlphaServer 2100 using SHELXL97.[28]

Crystal Structure Determination. Slow evaporation of a 10:1 benzene/MeCN (v/v) solution of [Pt(4,7-Me_2-php)Cl]CF_3SO_3 produced a pale orange needle of dimensions 0.40 × 0.23 × 0.05 mm that was suitable for diffraction studies. Least-squares refinement of the setting angles of 21386 reflections in the range $2° < \theta < 27°$ provided cell constants and an orientation matrix for the crystal mounted on a glass fiber. The maximum value of 2θ was 55.9°. There were 4767 unique reflections in the data set, and the average transmission coefficient was 0.614. The input for the refinement was the average of all equivalent reflections (agreement factor of 10.6%). The refinement took account of each of the unique reflections, but only data points that satisfied the criterion $F_o^2 > 2\sigma(F_o^2)$ were used in calculating the *R* value. Solution of the structure was done using the program PATTY in DIRDIF92.[29] Hydrogen atoms were included in the refinement with the constraint that they ride on the bonded atoms. Table 1 contains the key crystallographic data.

Computational Methodology. Geometries for php (C_s), 3,8-Me_2-php (C_s), 4,7-Me_2-php (C_s), 5,6-Me_2-php (C_s), trpy (C_{2v}), 1,-10-phenanthroline (C_{2v}), and pyridine (C_{2v}) were optimized (frozen-core approximation) at the Moller−Plesset (MP2) level of theory

(23) Eggleston, M. K.; McMillin, D. R.; Koenig, K. S.; Pallenberg, A. J. *Inorg. Chem.* **1997**, *36*, 172−176.

(24) Lakowicz, J. R. *Principles of Fluorescence Spectroscopy*, 2nd ed.; Kluwer Academic: Plenum: New York, 1999; p 52.

(25) Parker, C. A.; Rees, W. T. *Analyst (London)* **1960**, *85*, 587−600.

(26) Van Houten, J.; Watts, R. J. *J. Am. Chem. Soc.* **1975**, *97*, 3843−3844.

(27) Cunningham, K. L.; Hecker, C. R.; McMillin, D. R. *Inorg. Chim. Acta* **1996**, *242*, 143−147.

(28) Sheldrick, G. M. *SHELX97. A Program for Crystal Structure Refinement*; University of Göttingen: Göttingen, 1997.

(29) Beurskens, P. T.; Beurskens, G.; Garcia-Granda, R.; Gould, R. O.; Israel, R.; Smits, J. M. M. *The DIRDIF-99 Program System*; Crystallography Laboratory, University of Nijmegen: Nijmegen, 1999.

Table 1. Crystal Data and Collection Parameters for [Pt(4,7-Me_2-php)Cl]CF_3O_3S

formula	$C_{20}H_{15}ClF_3N_3O_3PtS$
fw	664.96
space group	$P2_1/n$ (No. 14)
a, Å	7.4316(3)
b, Å	13.6633(7)
c, Å	20.1448(12)
β, deg	96.5965(19)
V, Å^3	2032.0(3)
Z	4
d_{calc}, g cm^{-3}	2.174
cryst dimens, mm	0.40 × 0.23 × 0.05
temp, K	150
radiation (wavelength)	Mo Kα (0.71073 Å)
monochromator	graphite
linear abs coeff, mm^{-1}	7.263
abs correction applied	empirical[a]
transm factors: min, max	0.32, 0.70
diffractometer	Nonius KappaCCD
h, k, l ranges	0 to 9, 0 to 17, −26 to 26
2θ range, deg	5.05−55.86
mosaicity, deg	1.05
programs used	SHELXL-97
F_{000}	1272.0
weighting	$1/[\sigma^2(F_o^2) + (0.0552P)^2 + 0.0000P]$ where $P = (F_o^2 + 2F_c^2)/3$
data collected	21386
unique data	4767
R_{int}	0.106
data used in refinement	4761
R-factor cutoff	$F_o^2 > 2.0\sigma(F_o^2)$
data with $I > 2.0\sigma(I)$	2690
refined extinction coeff	0.0021
no. of variables	292
largest shift/esd in final cycle	<0.00
R(F_o)	0.053
$R_w(F_o^2)$	0.113
GOF	0.950

[a] Otwinowski, Z.; Minor, W. *Methods Enzymol.* **1996**, *276*, 307.

using the 6−31G(d,p) basis set.[30] All calculations were carried out with the Gaussian 98 electronic structure program suite.[31]

Results

Electrochemistry. Like platinum(II) terpyridines,[10,17] the Pt(php)Cl$^+$ systems exhibit two, ostensibly ligand-based reduction waves about 0.6 V apart in DMF (Table 2). Ligand reduction occurs at a more cathodic potential for the Zn(php)Cl_2 analogues, again in keeping with results for complexes involving terpyridine ligands.[17] For example, the potential for the reduction of Zn(php)Cl_2 is 0.55 V more negative than that of Pt(php)Cl$^+$. The reduction potential is ca. 0.2 V more positive for coordinated php compared to coordinated trpy. In accordance with an electron-donating effect, however, adding methyl substituents to the php ligand induces small negative shifts in the reduction potential (Table 2). The effect is larger for ring substitution at the 4,7-positions in comparison with the 3,8- or the 5,6-positions.

Table 2. Electrochemical Data from DMF Solutions at Room Temperature

NNN	Pt(NNN)Cl$^+$ E_1, V vs Fc$^{+/0}$	Pt(NNN)Cl$^+$ E_2, V vs Fc$^{+/0}$	Zn(NNN)Cl_2 E_0, V vs Fc$^{+/0}$
php	−1.09 (90, 1.1)[a]	−1.69 (60, 1.0)[a]	−1.64 (80, 1.2)[a]
4,7-Me_2-php	−1.17 (160, 1.3)	−1.76 (60, 1.2)	−1.68 (70, 1.3)
3,4,7,8-Me_4-php	−1.18 (210, 1.2)	−1.77 (60, 1.2)	−1.77 (90, 1.2)
5,6-Me_2-php	−1.13 (170, 1.2)	−1.75 (90, 1.1)	*b*
3,5,6,8-Me_4-php	−1.14 (190, 1.2)	−1.77 (50, 1.1)	*b*

[a] $E_{p,a} - E_{p,c}$ separation in mV and i_c/i_a current ratios in parentheses. [b] Not measured due to poor solubility.

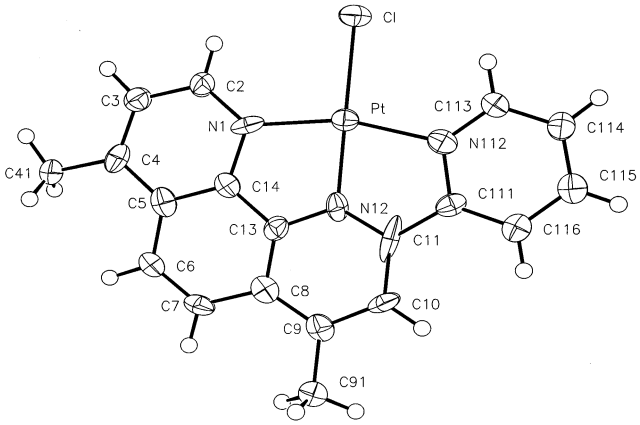

Figure 1. ORTEP[32] representation and crystallographic-numbering scheme for Pt(4,7-Me_2-php)Cl$^+$. The probability level for the thermal ellipsoids is 50%.

Table 3. Selected Structural Data for [Pt(4,7-Me_2-php)Cl]CF_3SO_3

	Bond Distances (Å)		
Pt−N1	2.013(8)	C5−C14	1.395(12)
Pt−N12	1.949(8)	C13−C14	1.410(13)
Pt−N112	2.025(8)	C9−C91	1.490(13)
Pt−Cl	2.302(2)	C4−C41	1.480(13)
C11−C111	1.426(16)	C111−N112	1.407(12)
C5−C6	1.457(13)	N112−C113	1.324(11)
C6−C7	1.357(14)	C113−C114	1.387(13)
C7−C8	1.424(13)	C114−C115	1.378(14)
C8−C13	1.405(13)	C115−C116	1.396(13)
	Angles (deg)		
N1−Pt−N12	82.4(3)	N112−Pt−Cl	99.2(2)
N12−Pt−N112	80.3(3)	N12−Pt−Cl	178.8(2)
N1−Pt−N112	162.7(3)	N12−C13−C14	115.1(9)
N1−Pt−Cl	98.1(2)	N12−C11−C111	114.8(12)

Structure of [Pt(4,7-Me_2-php)Cl]O_3SCF_3. The ORTEP[32] drawing in Figure 1 reveals the crystallographic-numbering scheme for the 4,7-Me_2-php ligand as well as the planar coordination geometry about platinum. Table 3 contains a listing of important bond angles and bond distances. In the crystal the cations stack in head-to-tail fashion in zigzag columns that angle off the crystallographic *a* axis. Alternating between 4.331(1) and 4.397(1) Å, the Pt−Pt separations are too long for any significant metal−metal interactions. Uncoordinated anions distribute in spaces between columns.

(30) Hariharan, P. C.; Pople, J. A. *Theor. Chim. Acta* **1973**, *28*, 213−222.
(31) Frisch, M. J.; Trucks, G. W.; Schlegel, H. B.; Scuseria, G. E.; Robb, M. A.; Cheeseman, J. R.; Zakrzewski, V. G.; Montgomery, J. J. A.; Stratmann, R. E.; Burant, J. C.; Dapprich, S.; Millam, J. M.; Daniels, A. D.; Kudin, K. N.; Strain, M. C.; Farkas, O.; Tomasi, J.; Barone, V.; Cossi, M.; Cammi, R.; Mennucci, B.; Pomelli, C.; Adamo, C.; Clifford, S.; Ochterski, J.; Petersson, G. A.; Ayala, P. Y.; Cui, Q.; Morokuma, K.; Malick, D. K.; Rabuck, A. D.; Raghavachari, K.; Foresman, J. B.; Cioslowski, J.; Ortiz, J. V.; Baboul, A. G.; Stefanov, B. B.; Liu, G.; Liashenko, A.; Piskorz, P.; Komaromi, I.; Gomperts; R. Martin, R. L.; Fox, D.; J. Keith, T.; Al-Laham, M. A.; Peng, C. Y.; Nanayakkara, A.; Gonzalez, C.; Challacombe, M.; Gill, P. M. W.; Johnson, B.; Chen, W.; Wong, M. W.; Andres, J. L.; Head-Gordon, M.; Replogle, E. S.; Pople, J. A. *Gaussian 98*; Gaussian, Inc.: Pittsburgh, PA, 1998.
(32) Johnson, C. K. *ORTEP II*; Oak Ridge National Laboratory: Oak Ridge, TN, 1976.

Table 4. Absorbance Data for Complexes of php and Related Ligands with Pt(II), Zn(II), and Fe(II) in Room-Temperature Solution

	λ_{max}, nm (absorbance)		
NNN	$Pt(NNN)Cl^{+}$ [a]	$Zn(NNN)Cl_2$ [a]	$Fe(NNN)_2^{2+}$ [b]
php	264, 305, 325, 345sh, 405sh, 421 [2600][c]	305, 328, 343, 358	440sh, 480, 535sh, 580
4,7-Me_2-php	263, 302, 320, 338s, 345sh, 395sh, 415 [3600]	305, 328, 342, 358	440sh, 485, 540, 590
3,4,7,8-Me_4-php	269, 290sh, 301, 326, 330sh, 405, 423 [3600]	305, 330, 344, 361	440sh, 480, 545sh, 595
5,6-Me_2-php	265, 302, 318sh, 329, 362, 415 [3900], 437sh	314, 342, 360, 379sh	440sh, 480, 530sh, 575
3,5,6,8-Me_4-php	264, 304, 330, 357sh, 416 [3800], 437sh	315, 341, 356, 372	440sh, 475, 540sh, 585

[a] In methylene chloride solution. [b] In water. [c] Molar absorptivity (M^{-1} cm^{-1}) in brackets.

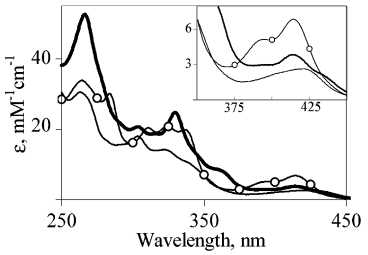

Figure 2. Absorption spectra of $Pt(4'\text{-Ph-T})Cl^{+}$ (−○−), $Pt(php)Cl^{+}$ (—), and $Pt(5,6\text{-}Me_2\text{-php})Cl^{+}$ (—, thick) in DCM solution at room temperature. Inset: Expansion of long-wavelength region.

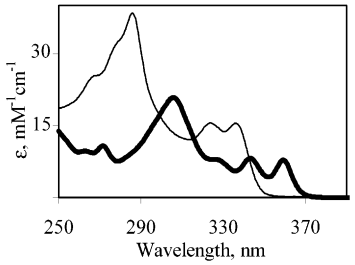

Figure 3. Absorption spectra of $Zn(4'\text{-Ph-T})Cl_2$ (—) and $Zn(php)Cl_2$ (—, thick) in DCM solution at room temperature.

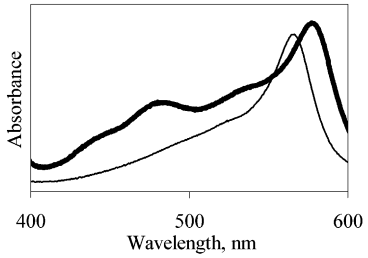

Figure 4. Visible spectra of $Fe(4'\text{-Ph-T})_2^{2+}$ (thin line) and $Fe(php)_2^{2+}$ (thick line) in water at room temperature.

The 4,7-Me_2-php ligand itself is essentially planar, and, within experimental error, the mean planes of the C111−C116 pyridine moiety and the N1−C14 phenanthroline core are coplanar. The average Pt−N bond distance is very similar in $Pt(4,7\text{-}Me_2\text{-php})Cl^{+}$ and $Pt(trpy)Cl^{+}$; however, the spread is greater in the trpy complex where the Pt−N distances are 1.93, 2.108, and 2.030 Å.[6] In contrast, the two Pt−Cl bond distances are virtually identical. Geometric constraints prevent tridentate ligands like trpy from achieving ideal bonding with a metal center,[7,33] and bond angles within the coordinated 4,7-Me_2-php ligand reveal the strain that occurs, especially within the pyridine moiety. Compare, for example, bond angles at C111 and C14: ∠(C11−C111−C116) = 127.0(9)° vs ∠(C13−C14−C5) = 120.3(9)°, and ∠(C116−C111−N112) = 118.2(9)° vs ∠(C5−C14−N1) = 123.3-(9)°. In the 4,7-Me_2-php complex, the N−Pt−N angle relating the terminal nitrogen donors is 162.7 (3)° compared with 161.8 (2)° in the trpy complex.

Absorption Spectra. The UV spectrum of $Pt(php)Cl^{+}$ exhibits two groups of bands analogous to those observed for the well-studied $Pt(trpy)Cl^{+}$ system (Figure 2).[7] First, a set of relatively intense, $\pi-\pi^*$ intraligand absorptions occur between 250 and 300 nm. A second, more highly structured series of intraligand $\pi-\pi^*$ absorptions occur in the 300−350 nm range. Figure 3 shows that analogous intraligand $\pi-\pi^*$ absorption bands appear in the spectra of $Zn(4'\text{-Ph-T})Cl_2$ and $Zn(php)Cl_2$, but at distinctly longer wavelengths for the php complex. Data in Table 4 show that incorporating methyl substituents typically has little effect on the energy of the intraligand absorptions except for substitution at the 5,6-positions. More specifically, the $\pi-\pi^*$ absorptions of $Zn(5,6\text{-}Me_2\text{-php})Cl_2$ and $Zn(3,5,6,8\text{-}Me_4\text{-php})Cl_2$ shift to longer wavelengths, and there is evidence of band broadening.

Lower energy bands, centered around 420 nm in the spectra of the platinum(II) analogues, are attributable to metal-to-ligand charge-transfer (MLCT) absorptions (Figure 2). The CT absorption of $Pt(php)Cl^{+}$ shows two poorly resolved components, separated by ca. 1100 cm^{-1}, which may correspond to vibronic structure. The longer wavelength component exhibits greater absorption intensity in the case of the php and 3,4,7,8-Me_4-php complexes, but the pattern reverses when there are methyl groups in the 5,6-positions (Figure 2). From complex to complex, the energy shifts are fairly small in the CT region, but introduction of methyl groups at the 5,6-positions of the phenanthroline core induces a shift toward longer wavelength. Related CT absorptions occur in the spectrum of $Fe(php)_2^{2+}$ but at lower energies due to the ease of oxidation of Fe(II) (Table 4). A second group of CT transitions is also relatively prominent in the region of 440−480 nm in the spectrum of $Fe(php)_2^{+}$ (Figure 4). The principal CT maximum occurs at 576 nm, and a shoulder at ca. 530 nm may represent vibrational structure and/or a splitting of the dπ orbitals of the metal center.[34,35] Figure 4 also reveals that similar structure appears in the absorption spectrum of $Fe(4'\text{-Ph-T})_2^{2+}$. The CT absorption of $Fe(php)_2^{2+}$ shifts to lower energy upon the introduction

(33) Figgis, B. N.; Kucharski, E. S.; White, A. H. *Aust. J. Chem.* **1983**, *36*, 1563−1571.

(34) Ceulemans, A.; Vanquickenborne, L. G. *J. Am. Chem. Soc.* **1981**, *103*, 2238−2241.

(35) Seneviratne, D. S.; Uddin, J.; Swayambunathan, V.; Schlegel, H. B.; Endicott, J. F. *Inorg. Chem.* **2002**, *41*, 1502−1517.

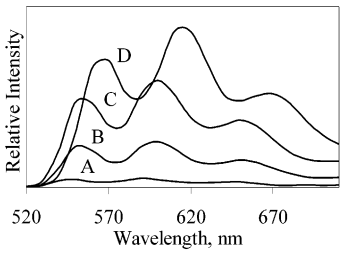

Figure 5. Corrected emission spectra of Pt(php)Cl^+ complexes in DCM solution at room temperature. The absorbance at the excitation wavelength is the same for (A) Pt(php)Cl^+, (B) Pt(4,7-Me_2-php)Cl^+, (C) Pt(3,4,7,8-Me_4-php)Cl^+, and (D) Pt(3,5,6,8-Me_4-php)Cl^+.

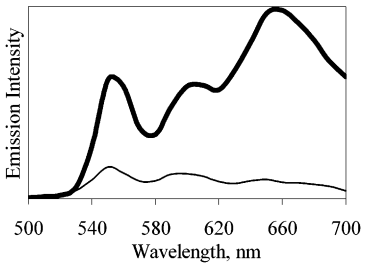

Figure 6. Corrected emission spectrum of Pt(5,6-Me_2-php)Cl^+ in butyronitrile at 77 K. The platinum concentrations are 1.7 μM (thin line) and 17 μM (thick line).

Table 5. Data from Corrected Emission Spectra of Pt(php)Cl^+ and Related Systems in Deoxygenated Dichloromethane Solution at Room Temperature

Ligand	λ_{max}, nm	τ, μs	$10^2\phi$	k_r, s^{-1}
php	547, 591, 650	0.23	0.31	1.2×10^4
4,7-Me_2-php	553, 599, 653	1.5	1.6	1.1×10^4
3,4,7,8-Me_4-php	554, 601, 655	4.0	3.8	9.4×10^3
5,6-Me_2-php	563, 609, 673	5.0	2.6	5.3×10^3
3,5,6,8-Me_4-php	567, 611, 675	9.3	5.5	6.0×10^3

of methyl substituents at the 3,8- or 4,7-positions, while substitution at the 5,6-positions shifts the absorption in the opposite direction (Table 4).

Emission Data. The Pt(php)Cl^+ systems exhibit relatively intense, structured emission spectra in room-temperature DCM solution (Figure 5). The short wavelength maximum at 545 nm in the corrected emission spectrum of the parent php complex is the 0−0 transition that connects the ground vibrational levels of the two participating electronic states. Under a nitrogen atmosphere, the php complex exhibits an emission quantum yield of 3.1×10^{-3} and an excited-state lifetime of 0.23 μs at room temperature. For comparison, the analogous Pt(4′-Ph-T)Cl^+ system has a 0−0 emission band at 535 nm and an excited-state lifetime of 85 ns.[11,12] Incorporating methyl substituents into the Pt(php)Cl^+ system enhances the lifetime and the quantum yield despite the fact that the emission shifts to lower energy (Table 5). Substitution at the 5,6-positions is most effective, and the 3,5,6,8-Me_4-php system exhibits the highest emission yield (0.055) and the longest excited-state lifetime (9.3 μs) in the series.

As is the case with trpy analogues,[8,9] the emission from low-temperature glasses containing Pt(php)Cl^+ is very concentration dependent. The broad, intense emission evident at longer wavelengths in concentrated solutions is attributable to aggregated forms of the luminophore; see ref 9. In Figure 6 the corrected emission spectrum from the dilute glass is probably representative of a monomeric platinum(II) system.

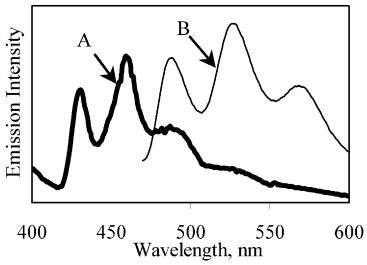

Figure 7. Corrected emission spectra of (A) Zn(4′-Ph-T)Cl_2 and (B) Zn(php)Cl_2 in ethylene glycol at 77 K.

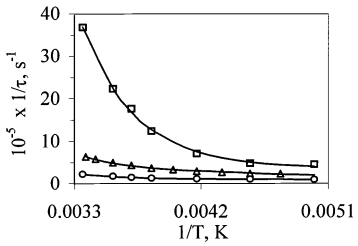

Figure 8. Temperature-dependent decay rates measured in DCM for Pt(php)Cl^+ (□), Pt(4,7-Me_2-php)Cl^+ (△), and Pt(5,6-Me_2-php)Cl^+ (○). The curves are the best fits of the data to eq 1.

Table 6. Data from Corrected Emission Spectra of php and Related Complexes of Pt(II) and Zn(II) in Rigid Glasses at 77 K

NNN	Pt(NNN)Cl^+ in butyronitrile λ_{max}, nm	Zn(NNN)Cl_2 in ethylene glycol λ_{max}, nm	Zn(NNN)Cl_2 in ethylene glycol τ, s
php	533, 576, 631	489, 528, 572	0.93
4,7-Me_2-php	540, 587, 640	498, 538, 582	0.89
3,4,7,8-Me_4-php	545, 591, 643	500, 539, 583	1.0
5,6-Me_2-php	558, 608	523, 563, 612	0.76
3,5,6,8-Me_4-php	561, 610, 665	522, 563, 612	0.87

The band shape of the emission from the monomeric component is qualitatively similar to that observed in fluid solution, except that there is a small shift toward shorter wavelength in the low-temperature matrix. For reference, Figure 7 includes the frozen solution emission spectrum of the Zn(php)Cl_2 complex, and Table 6 includes data for analogous methyl-substituted php derivatives. The emissions from the zinc systems occur at higher energies but show the same kind of vibrational structure. Here, too, introduction of methyl substituents induces a bathochromic shift in the emission, but substituents have comparatively little influence on the emission lifetime within the zinc series, at least at 77 K (Table 6).

The data in Figure 8 reveal that the decay rate has a weak temperature dependence in DCM solution for Pt(php)Cl^+ derivatives when the excited-state lifetime is of the order of a microsecond at room temperature. However, the decay rate falls off rapidly for the Pt(php)Cl^+ system at lower temperatures. A fit of the data to the equation

$$k = k_1 \exp(\Delta E/RT) + k_0 \qquad (1)$$

gives a ΔE of 1840 cm^{-1} and a preexponential factor of 2.3×10^{10} s^{-1} for the php system. The ΔE is a reasonable value for thermal population of a higher energy d−d state. It is probably coincidental that the fits for the 4,7-Me_2-php and

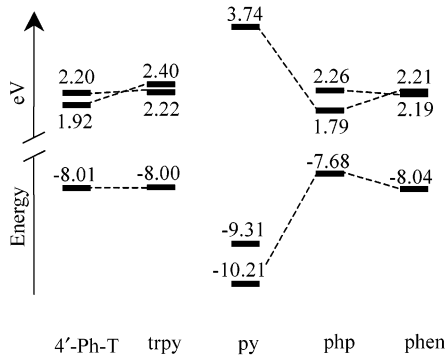

Figure 9. Calculated energies for the frontier orbitals of 4′-Ph-T, trpy, pyridine, php, and 1,10-phenanthroline. The LUMO and LUMO+1 orbitals all have positive energies while the energies are negative for the HOMO and HOMO−1 orbitals.

5,6-Me_2-php systems give similar ΔE values of 1380 and 1580 cm^{-1}, respectively. For these systems the thermally assisted decay process is much less efficient and probably does not relate to population of a d−d state. According to the fits, the limiting lifetimes (k_0^{-1} values) are 3, 5, and 11 μs for the php, 4,7-Me_2-php, and 5,6-Me_2-php systems, respectively.

The emission results establish two distinct solvent effects. The first is that donating solvents (Lewis bases) quench the emission. In every case, quenching is essentially complete in DMF at room temperature. In the less basic solvent acetonitrile, the emission from photoexcited Pt(5,6-Me_2-php)Cl^+ persists with a lifetime of 98 ns while the residual emission from Pt(3,5,6,8-Me_4-php)Cl^+ has a slightly longer decay time of 164 ns. The more surprising observation is that the addition of noncoordinating toluene also attenuates the emission signal. As described above, the photoluminescence of Pt(5,6-Me_2-php)Cl^+ decays with a lifetime of 5.0 μs in deoxygenated DCM solution. When the solution contains 10 vol % toluene, the lifetime drops to 1.25 μs, independent of the platinum concentration in the range 0.46−46 μM. Moreover, in the same solvent mixture the addition of up to a 100-fold excess of the tetramethylammonium salt of the TFPB anion has no effect on the lifetime. In 50 vol % toluene, the lifetime is even shorter at 420 ns, again independent of the platinum concentration in the range 10−100 μM. In 75% toluene the lifetime is only 330 ns.

MO Calculations. Figure 9 shows how the frontier orbitals of php correlate with those of the parent compounds, pyridine and 1,10-phenanthroline. The mixing of the LUMO of pyridine with the LUMO+1 of 1,10-phenanthroline results in a relatively low-energy LUMO for php. In addition, php has a relatively high energy HOMO due to the mixing of the HOMO−1 of pyridine with the HOMO of 1,10-phenanthroline. As a result, php has the narrowest HOMO−LUMO gap of the five ligands in Figure 9. Figure 10 shows the relative magnitudes of the p(π) atomic orbitals on the carbon and nitrogen atoms for the HOMO and LUMO of php. In accordance with the frontier orbital energies of pyridine and 1,10-phenanthroline (Figure 9), it is not surprising that most of the amplitude of the HOMO and LUMO orbitals of php resides on the 1,10-phenanthroline end of the molecule.

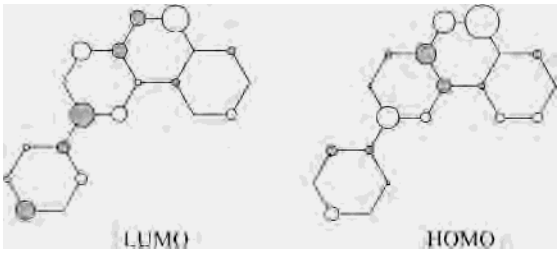

Figure 10. Frontier orbitals of php. The radius of the circle indicates the relative participation of a particular p(π) atomic orbital. Shaded circles depict negative amplitudes.

For php, the MO calculations also show that the p(π) atomic orbital of the central nitrogen atom makes a significant contribution to the LUMO+1. In contrast, this same orbital coefficient is equal to zero in the LUMO+1 for trpy. This is a significant difference between the two ligands because the involvement of the p(π) orbital of nitrogen is essential for the development of oscillator strength for CT absorption.[34,36,37] Indeed, the CT transitions that occur between 400 and 500 nm in the spectrum of Fe(php)$_2^{2+}$ probably involve excitation into the LUMO+1 orbital of php, and it is not surprising that the analogous transitions of Fe(4′-Ph-T)$_2^{2+}$ are much weaker (Figure 4). Finally, the two types of CT transitions are likely to be less resolved for Fe(4′-Ph-T)$_2^{2+}$ because the difference in energy between the LUMO and LUMO+1 is smaller in the case of the 4′-Ph-T ligand.

Because the X-ray structure of Pt(4,7-Me_2-php)Cl^+ indicates that the 4,7-Me_2-php ligand is essentially planar, the MP2 calculations for this ligand, as well as the 3,8-Me_2-php and 5,6-Me_2-php ligands, were carried out using C_s symmetry constraints. Of course, there are four possible C_s structures (rotamers) for each ligand. For the 4,7-Me_2-php ligand, the lowest energy rotamer has the two in-plane, methyl C−H bonds oriented toward C3 and C8 of the 1,10-phenanthroline group. The X-ray data are also consistent with this conformation. The calculated distances between the in-plane, methyl hydrogens and the hydrogen atoms at C3 and C8 are 2.37 and 2.32 Å, respectively. At 0.17 eV higher energy, the least stable rotamer has the two in-plane, methyl C−H bonds oriented toward C5 and C6 of the 1,10-phenanthroline group. For this structure, the closest (MP2 calculated) distances between the in-plane, methyl hydrogens and the C5 and C6 hydrogens are 1.97 and 1.98 Å. The total energies of the other two C_s rotamers of 4,7-Me_2-php fall almost exactly halfway between these two extremes. In the case of the 5,6-Me_2-php ligand, MP2 calculations indicate that the "head-to-head" arrangement of the in-plane, methyl hydrogens has the lowest energy even though the hydrogen atoms are calculated to be only 1.86 Å apart. The "tail-to-tail" rotamer has the highest energy and a calculated separation of 1.91 Å between the in-plane hydrogen of the C6 methyl group and the neighboring C7 hydrogen.

In most cases, the presence of methyl substituents affects the HOMO and LUMO energies. The HOMO shifts from

(36) Day, P.; Sanders, N. *J. Chem. Soc. A* **1967**, 1536−1541.
(37) Phifer, C. C.; McMillin, D. R. *Inorg. Chem.* **1986**, *25*, 1329−1333.

−7.68 eV for php to −7.59, −7.53, and −7.52 eV for the most stable rotamers of 3,8-Me_2-php, 4,7-Me_2-php, and 5,6-Me_2-php, respectively. There is less of a trend in the LUMO energies which are 1.79, 1.86, 1.79, and 1.88 eV for php, 3,8-Me_2-php, 4,7-Me_2-php, and 5,6-Me_2-php, respectively. Methyl substituents also appear to destabilize the nitrogen-based n(σ) orbital that has the appropriate symmetry to interact with the d(σ) orbital of platinum. For example, this orbital shifts from −10.58 eV in php to −10.31 eV in 3,8-Me_2-php.

Discussion

Photophysics of Pt(php)Cl$^+$. The observation of emission from Pt(php)Cl$^+$ at room temperature in DCM solution is quite intriguing because radiationless decay via low-lying d−d states is often extremely efficient in platinum(II) complexes.[38] Indeed, this process explains why the analogous Pt(trpy)Cl$^+$ system is nonluminescent.[1,7] However, the Pt(4′-Ph-T)Cl$^+$ complex provides an interesting contrast in that the complex is emissive and exhibits an excited-state lifetime of 85 ns in deoxygenated DCM solution.[12] One possible explanation is that extended conjugation within the 4′-Ph-T ligand reduces the degree of distortion in the excited state and thereby enhances the intrinsic lifetime.[39] More likely, the presence of the phenyl substituent leads to a lower energy CT excited state and a higher barrier to deactivation via d−d excited states.[1,12] The Pt(php)Cl$^+$ system also appears to have a relatively low energy excited state because it has a CT absorption maximum of 421 nm in DCM solution versus 405 nm for Pt(trpy)Cl$^+$.[7] MO calculations help explain the difference because the π^* LUMO is about 0.5 V lower in energy for php compared with trpy (Figure 9). Electrochemical data are also consistent with the expected trend in LUMO energies. The most straightforward comparison of ligand reduction involves a comparison of zinc(II) analogues. While reduction of Zn(trpy)Cl_2 takes place at −1.86 V vs $Fc^{+/0}$, reduction of the php complex occurs at a less cathodic potential of −1.64 V (versus the same reference). The data in Figure 8 indicate that thermally activated deactivation occurs in Pt(php)Cl$^+$; the process is just more efficient in Pt(trpy)Cl$^+$.

The results discussed so far clearly establish roles for d−d and CT excited states in shaping the basic photophysical properties of Pt(php)Cl$^+$ and related systems; however, several observations remain unexplained. One is that the rigidity of the php ligand can also lead to low-energy d−d excited states as is the case with the Ru(php)$_2^{2+}$ system which is nonluminescent in solution.[40] Why should the platinum analogue behave differently? Methyl substituents influence the CT absorption maxima of Fe(php)$_2^{2+}$ derivatives in a positionally dependent way (Table 4). Why do the emission maxima of the Pt(php)Cl$^+$ not follow the same pattern? Contrary to expectations based on the energy-gap law,[41−43] data in Table 5 show that the lifetime in the series of php complexes increases as the emission energy decreases. Why does the addition of methyl substituents have such an effect? Finally, why is the vibrational structure in the emission spectrum of Pt(php)Cl$^+$ so much more pronounced than that observed for trpy-based systems like Pt(4′-CN-T)Cl$^+$,[10] where 4′-CN-T denotes 4′-cyano-2,2′:6′,2″-terpyridine?

Other Proximate States. The answers to all these questions revolve around variations in orbital parentage. In principle, several types of excitation can cooperate, including d−p excitation. Thus, Gray and co-workers have pointed out that the accessibility of the empty platinum $6p_z$ orbital may account for the anomalously easy reduction of platinum(II) polypyridine complexes by comparison with zinc(II) analogues.[17] However, d−p excitation typically falls at around 250 nm in the absorption spectrum,[44] so it probably has little bearing on the much lower energy emitting states. Intraligand charge-transfer excited states can also occur in Pt(trpy)Cl$^+$ derivatives, but this requires the presence of electron-rich substituents like dialkylamines or large, fused-ring aryl substituents, such as 1-pyrenyl.[10,12]

What turns out to be a comparatively low energy process in the php system is intraligand $\pi-\pi^*$ excitation. Thus, the first absorption in the electronic spectrum of Zn(php)Cl_2 occurs at 358 nm compared with 335 nm for Zn(4′-Ph-T)-Cl_2.[12] Furthermore, data in Table 4 establish that the $\pi-\pi^*$ absorption shifts to even longer wavelength with the addition of methyl substituents. Although the lowest energy electronic transitions in polycyclic aromatic compounds are not always well described as HOMO to LUMO excitations,[45] this gap is still a fundamental determinant of the $\pi-\pi^*$ transition energies. The comparison of the HOMO−LUMO gaps for php and 4′-Ph-T in Figure 9 is quite revealing. The greater HOMO−LUMO separation for 4′-Ph-T may be a result of the fact that the meta linkages in 4′-Ph-T prevent conjugation across the central ring.[46] MP2 calculations also indicate that the 4′-phenyl substitutent has little impact on the HOMO or the LUMO orbital of the trpy core because each of these orbitals has a node at the C4′ carbon.

Unfortunately, the MP2 calculations pertain to the ground state and do not provide much insight into the photophysics. In general, the impact a methyl substituent has on any particular energy level depends upon the orbital amplitude at the point of substitution.[47−49] This may explain why the

(38) Barigelletti, F.; Sandrini, D.; Maestri, M.; Balzani, V.; von Zelewsky, A.; Chassot, L.; Jolliet, P.; Maeder, U. *Inorg. Chem.* **1988**, *27*, 3644−3647.
(39) Damrauer, N. H.; Boussie, T. R.; Devenney, M.; McCusker, J. K. *J. Am. Chem. Soc.* **1997**, *119*, 8253−8268.
(40) Hung, C. Y.; Wang, T. L.; Jang, Y. C.; Kim, W. Y.; Schmehl, R. H.; Thummel, R. P. *Inorg. Chem.* **1996**, *35*, 5953−5956.
(41) Englman, R.; Jortner, J. *Mol. Phys.* **1970**, *18*, 145−164.
(42) Caspar, J. V.; Kober, E. M.; Sullivan, B. P.; Meyer, T. J. *J. Am. Chem. Soc.* **1982**, *104*, 630−632.
(43) Stufkens, D. J.; Vlcek, A., Jr. *Coord. Chem. Rev.* **1988**, *177*, 127−179.
(44) Connick, W. B.; Miskowski, V. M.; Houlding, V. H.; Gray, H. B. *Inorg. Chem.* **2000**, *39*, 2585−2592.
(45) Dewar, M. J. S.; Longuet-Higgins, H. C. *Proc. Phys. Soc. (London)* **1954**, *A67*, 795−804.
(46) Jaffe, H. H.; Orchin, M. *Theory and Applications of Ultraviolet Spectroscopy*; Wiley and Sons: New York, 1962; pp 273−276.
(47) Farrell, I. R.; Hartl, F.; Zalis, S.; Mahabiersing, T.; Vlcek, A. *J. Chem. Soc., Dalton Trans.* **2000**, 4323−4331.
(48) Klein, A.; Kaim, W.; Waldhor, E.; Hausen, H. D. *J. Chem. Soc., Perkin Trans. 2* **1995**, 2121−2126.
(49) Gouterman, M. *J. Chem. Phys.* **1959**, *30*, 1139−1161.

calculated decrease in the HOMO−LUMO gap is only 0.02 eV (9.47 eV to 9.45 eV) when substitution occurs at the C3 and C8 positions of the phenanthroline where the orbital coefficients are vanishingly small for the two frontier orbitals of php. On the basis of the spectral data from the zinc compounds, one might expect the HOMO−LUMO gap to be smallest for the 5,6-Me_2-php derivative; however, theory predicts this ligand to have a HOMO−LUMO gap of 9.40 eV versus 9.32 eV for 4,7-Me_2-php.

Orbital Parentage of the Emission. There is no question about the CT character of the lowest energy absorption bands of Pt(php)Cl^+, but the same state assignment need not apply to the emissions. The multiplicity is clear because the lifetimes and the calculated radiative rate constants in Table 5 are only consistent with emission from a triplet excited state, albeit one involving a heavy metal center. However, the lowest energy triplet state could have intraligand excited-state character because the singlet−triplet splitting is typically much larger for $\pi-\pi^*$ as compared with CT excitation.[50,51] Indeed, the vibrational structure in the emission spectra in Figure 5 provides evidence of substantial $^3\pi-\pi^*$ character. Vibrational spacings of ca. 1400 cm^{-1} implicate C=C and/or C=N double-bond stretching modes, and the fact that there are relatively long progressions establishes that the ligand framework has a different geometry in the excited state. In principle, either $d-\pi^*$ or $\pi-\pi^*$ excitation would give rise to an expansion of the ligand framework due to the population of an intraligand antibonding orbital. However, the 0−0 transition would be the most intense component in emission from a $d-\pi^*$ excited state. Dome-shaped intensity distributions, like those in Figure 5, are indicative of a relatively large shift in equilibrium geometry. This is more consistent with $\pi-\pi^*$ excitation because the depopulation of an intraligand bonding orbital is also a factor.[52,53]

Nevertheless, $d-\pi^*$ excitation must play a role. A radiative rate constant of the order of 10^4 s^{-1} is simply not feasible for a pure $^3\pi-\pi^*$ excited state when spin remains a good quantum number. An admixture of $d-\pi^*$ (CT) character eases this restriction due to participation of orbitals of the heavy metal center.[14,54,55] A mixed orbital parentage can also account for the fact that the emission spectra of the Pt(php)-Cl^+ derivatives have lower 0−0 transitions than the Zn(php)-Cl_2 analogues. Pure $^3\pi-\pi^*$ emission would occur at essentially the same energy.[14] The fact that the emission from Pt(5,6-Me_2-php)Cl^+ shows modest rigidochromism, i.e., a blue shift in frozen solution, is also consistent with the emission having some degree of $d-\pi^*$ character.[56] Thus, at room temperature in acetonitrile solution, the 0−0 transition occurs at 560 nm in the corrected emission spectrum versus 550 nm in butyronitrile at 77 K. Finally, systematic variations in the amount of $^3d-\pi^*$ participation account for otherwise perplexing substituent effects. Consider the lifetimes. They vary dramatically within the platinum complexes, but there is very little change among the $^3\pi-\pi^*$ lifetimes of the Zn-(php)Cl_2 series at 77 K. For the platinum complexes, the efficiency of thermal deactivation from higher energy d−d excited states varies somewhat at room temperature, but the trend in lifetimes actually remains the same down to 200 K for the Pt(5,6-Me_2-php)Cl^+, Pt(4,7-Me_2-php)Cl^+, Pt(php)-Cl^+ series. The obvious explanation is that the addition of methyl substituents induces a drop in the energy of $^3\pi-\pi^*$ excitation and thereby enhances its contribution to the excited-state character. In line with this explanation, the k_r values generally decrease as the emission energy decreases (Table 5). Once again, substitution at the 5,6-positions of the phenanthroline is most effective, and that explains why the 5,6-Me_2-php and 3,5,6,8-Me_4-php complexes have similar radiative rate constants. The Watts and Crosby groups have found that a related kind of excited-state tuning occurs in mixed-ligand iridium complexes.[57,58] In their systems, which also exhibit $^3\pi-\pi/^3d-\pi^*$ emissions, it is possible to alter the orbital parentage by changing the solvent which affects the energy of the polar $^3d-\pi^*$ component.

There are at least two mechanisms through which formally intraligand $\pi-\pi^*$ excited states can take on d-orbital character in Pt(php)Cl^+ systems. One way is via covalent bonding. Due to favorable overlap of $d\pi$ orbitals of the metal with π and π^* orbitals of the ligand, the molecular orbitals of the complex naturally delocalize over both metal and ligand centers.[1,52] Because there are no σ-bonding interactions with axial ligands, the platinum $6p_z$ orbital is also available to participate in the mix.[17,44] Two-electron terms also help shape the electron distribution because incorporating multiple configurations generally provides for a decreased electron−electron repulsion energy.[59] When different configurations interact, the rule of thumb is that the extent of mixing varies inversely with the energy separation.[14] Configuration interaction is especially important among excited states because multiple excitations often have rather similar energies. The energetic analysis becomes even more complex when the states involved have different equilibrium geometries.[60] For the Pt(php)Cl^+ series, there are at least two distortion coordinates to consider. Thus, in addition to displacement along the intraligand breathing mode discussed above, one expects a $d-\pi^*$ state to distort along the metal−ligand stretching coordinate. Another complication is that the strength of coupling can also vary with the nature of the $d-\pi^*$ configuration involved.[44] The reason is that the interaction energy depends upon the exchange integral which can be small if the excitation originates in a $d\sigma$ orbital which has no net overlap with the π^* orbital of the ligand. In short,

(50) Michl, J.; Bonacic-Koutecky, V. *Electronic Aspects of Organic Photochemistry*; Wiley-Interscience: New York, 1990; pp 29−43.
(51) DePriest, J.; Zheng, G. Y.; Goswami, N.; Eichhorn, D. M.; Woods, C.; Rillema, D. P. *Inorg. Chem.* **2000**, *39*, 1955−1963.
(52) DeArmond, M. K.; Hillis, J. E. *J. Chem. Phys.* **1971**, *54*, 2247−2253.
(53) Indelli, M. T.; Bignozzi, C. A.; Marconi, A.; Scandola, F. *J. Am. Chem. Soc.* **1988**, *110*, 7381−7386.
(54) Ayala, N. P.; Flynn, C. M.; Sacksteder, L.; Demas, J. N.; Degraff, B. A. *J. Am. Chem. Soc.* **1990**, *112*, 3837−3844.
(55) Pierloot, K.; Ceulemans, A.; Merchan, M.; Serrano-Andres, L. *J. Phys. Chem. A* **2000**, *104*, 4374−4382.
(56) Wrighton, M. S.; Morse, D. L. *J. Organomet. Chem.* **1975**, *97*, 405−419.
(57) Watts, R. J.; Crosby, G. A.; Sansregret, J. L. *Inorg. Chem.* **1972**, *11*, 1474−1483.
(58) Cremers, T. L.; Crosby, G. A. *Chem. Phys. Lett.* **1980**, *73*, 541−544.
(59) Michl, J.; Bonacic-Koutecky, V. *Electronic Aspects of Organic Photochemistry*; Wiley-Interscience: New York, 1990; pp 442−462.
(60) Watts, R. J. *Inorg. Chem.* **1981**, *20*, 2302−2306.

Chart 2

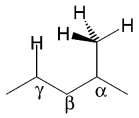

it is clear that $^3\pi-\pi/^3d-\pi^*$ configurational mixing occurs in the php systems, although a quantitative analysis is difficult. Moreover, the introduction of methyl substituents enhances intraligand character.

Methyl Orientation. Chart 2 depicts the favored orientation of the methyl rotors in the lowest energy structures calculated for 4,7-Me_2-php and 5,6-Me_2-php. Similar relationships occur in 1,5-dimethylnaphthalene. Wilson has shown that the out-of-plane hydrogens of the methyl groups of 1,5-dimethylnaphthalene strongly prefer to straddle the $C_\gamma-H$ bond in the solid state and has rationalized the result as a steric effect.[61] Wimmer and Müller invoke an ortho-substitution effect to explain an analogous rotational barrier.[62] For 5,6-Me_2-php, however, a "ball-and-stick" picture simply cannot account for the preferred conformation indicated from MP2 calculations. In these molecules electronic effects appear to be important. For example, hyperconjugative interactions between the out-of-plane methyl hydrogens and the p(π) orbital at C_γ probably play some role in determining the energetic ordering for the rotamers.

External Quenching. Previous work has established that associative attack by Lewis bases (exciplex quenching) is slow for a photoexcited Pt(trpy)Cl^+-like system when the lowest energy excited state has mainly intraligand orbital parentage.[1,63] As a consequence, Pt(5,6-Me_2-php)Cl^+ and Pt(3,5,6,8-Me_4-php)Cl^+ retain modest excited-state lifetimes in a weakly donating solvent like acetonitrile; however, neither complex exhibits emission in fluid solutions involving more basic solvents like DMF. The results are somewhat different with Cu(TPP), where TPP denotes the deprotonated form of 5,10,15,20-tetraphenylporphyrin.[64] Like Pt(5,6-Me_2-php)Cl^+, Cu(TPP) is a planar complex with a reactive excited state that involves intraligand excitation. However, the d^9 electronic configuration of Cu(II) presents a smaller barrier to ligand addition than a d^8, heavy-metal center with a large ligand-field splitting.[63] As a consequence, acetonitrile is more effective at quenching photoexcited Cu(TPP).

Introducing toluene into DCM solutions shortens the lifetime of photoexcited Pt(5,6-Me_2-php)Cl^+, but toluene itself is almost certainly not basic enough to induce exciplex quenching. However, counterion-induced quenching may be a solvent-dependent process. The fluorine atoms on the periphery of the TFPB anion are not very good donor centers, but they would become more reactive as the average hydrogen-bonding strength of the solvent decreases. For the charge-transfer excited state of the bis(2,9-dimethyl-1,10-phenanthroline)copper(I) ion, counterion-induced exciplex quenching has been shown to result in a concentration-dependent excited-state lifetime in DCM solution.[65] In contrast, the excited-state lifetime of the Pt(5,6-Me_2-php)Cl^+ system is independent of concentration in the accessible range of concentrations. If, however, the cations and anions largely exist as outer-sphere ion pairs in the low-dielectric medium, the concentration effect would be small. Despite outer-sphere complex formation, the combined influence of the d^8 configuration and the weakly nucleophilic anion could permit the excited state to persist for hundreds of nanoseconds. An alternative explanation for the quenching could be that electron transfer from the TFPB anion becomes less endoergic in a very nonpolar environment.

Conclusions and Comparisons

While Pt(trpy)Cl^+ has proven to be a convenient binding agent and spectral probe, Pt(php)Cl^+ promises to be more versatile because it exhibits similar CT absorption and is photoluminescent as well. *Theory reveals some fundamental limitations* of *the trpy framework*. One problem is restricted conjugation due to the meta relationship of the three pyridine rings. Another is that the HOMO and LUMO orbitals of the trpy ligand each have a nodal plane that bisects the central pyridine ring. Since available synthetic routes mostly yield 4′-substituted ligands, only strongly perturbing substituents can significantly impact the excited-state manifold. In contrast, the php ligand incorporates a fused-ring structure that gives rise to a π system with a relatively small HOMO−LUMO gap. As a consequence, the emissions from Pt(php)Cl^+ and related derivatives exhibit pronounced vibrational structure and a mixed $^3\pi-\pi^*/^3d-\pi^*$ orbital parentage. *An equally remarkable finding is the stereoelectronic influence that simple methyl substituents have on the photophysics*. Through substituent addition, one can tune the orbital parentage of the emitting state with dramatic impact. Whereas the parent complex Pt(php)Cl^+ has an excited-state lifetime of 0.23 μs in DCM solution, the lifetime increases 40-fold for the Pt(3,5,6,8-Me_4-php)Cl^+ analogue. The intraligand character of the excitation is important for the lifetime, while the $d-\pi^*$ CT character provides for a favorable radiative rate constant and the solvent sensitivity of the emission. Strong donor solvents like DMF are potent emission quenchers.

Acknowledgment. The National Science Foundation helped fund this research through Grant No. CHE 01-08902. Kurstan L. Cunningham first synthesized the php ligand in this laboratory. The authors thank J. B. Grutzner for helpful discussions. Michael H. Wilson carried out the quenching studies with the tetramethylammonium salt of the TFPB anion.

Supporting Information Available: Crystallographic data in CIF format. This material is available free of charge via the Internet at http://pubs.acs.org.

IC025922C

(61) Wilson, C. C. *Chem. Commun.* **1997**, 1281−1282.
(62) Wimmer, R.; Müller, N. *J. Magn. Reson.* **1997**, *129*, 1−9.
(63) Crites Tears, D. K.; McMillin, D. R. *Coord. Chem. Rev.* **2001**, *211*, 195−205.
(64) Liu, F.; Cunningham, K. L.; Uphues, W.; Fink, G. W.; Schmolt, J.; McMillin, D. R. *Inorg. Chem.* **1995**, *34*, 2015−2018.
(65) Everly, R. M.; McMillin, D. R. *Photochem. Photobiol.* **1989**, *50*, 711−716.